

Chitosan bio-functionalization of carbon nanotube arrayed electrode

Hadar Ben-Yoav^{1*}, Marshall A. Schroeder², Malachi Noked³

¹Department of Biomedical Engineering, Ben-Gurion University of the Negev, Beer Sheva, 8410501, Israel

²Sensor and Electron Devices Directorate, U.S. Army Research Laboratory, Adelphi, MD 20783, USA

³Department of Chemistry, Bar Ilan University, Ramat Gan, 52900, Israel

*Corresponding author: Tel: (+972) 8-6479717; E-mail: benyoav@bgu.ac.il

Received: 28 December 2016, Revised: 16 January 2017 and Accepted: 09 April 2017

DOI: 10.5185/amlett.2017.1577

www.vbripress.com/aml

Abstract

Nanostructured electrodes enable a new generation of electrochemical sensors by increasing their surface area that lead to stronger signals generated by electrochemically-active molecules, such as diagnostic redox-active biomarkers. Yet, the selectivity of these translational sensors is far from being sufficient for discriminating between individual molecules in multicomponent samples, such as biofluids. Here, we propose an approach to improve the selectivity of nanostructured electrodes using a simple modification with a functional bio-polymer. Specifically, we demonstrate the targeted modification with a bio-polymer chitosan of carbon nanotubes organized in an array on a Au electrode. We describe the fabrication process and we show the characterization of the structural morphology and the electrochemical activity of the fabricated chitosan-modified carbon nanotube arrayed electrode. Electrochemical characterization yielded an increased effective surface area for the optimized carbon nanotube arrayed electrode ($0.46 \pm 0.03 \text{ cm}^2$) that was similar to the area of the unmodified Au electrode ($0.48 \pm 0.02 \text{ cm}^2$). Furthermore, despite decreased electrochemical current characteristics, we demonstrate the feasibility to modify individual carbon nanotubes with chitosan. The modification of the carbon nanostructures with chitosan will enable further functionalization with specific receptors, such as enzymes and antibodies that will provide the required selectivity towards biomarkers in multicomponent biofluids. Copyright © 2017 VBRI Press.

Keywords: Electrochemical sensors, chitosan, carbon nanotubes, modified electrodes.

Introduction

Continuous monitoring of multiple diagnostic biological and chemical markers in biofluids can provide important and dynamic ‘biomolecular feedback’ about the physiological conditions of patients, thus enabling early disease detection and promoting personalized therapy [1-3]. However, most continuous monitoring approaches currently suffer from delayed responses and a long duration between diagnostic tests, which limit the ability of doctors and caregivers to rapidly adjust treatment or medication dosage. Thus, a more efficient scheme for such continuous monitoring requires the development of low-cost analytical micro-devices (“portable laboratories”), in which the sensor continuously measures the *in situ* levels of unlabeled redox-active diagnostic markers in the sample [4, 5]. Recent advancements suggest that miniaturized, electrochemical sensors, which generate a unique electronic signal according to the redox potential of a molecule of interest, are well suited for this analytical task [6-9]. However, when the concentration of the diagnostic marker are low and several other redox-active molecules in the sample generate overlapping electrochemical signals, the electrochemical sensor must

be able to detect the marker within the required diagnostic levels [10, 11].

An effective approach to increase the electrochemical signal generated by the redox-active marker entails the modification of the electrode with semi-selective films that can be designed to influence the redox reaction so as to better control the electron transfer rates of a molecule of interest at the expense of another molecule [12-15]. The works of Tiwari, Katz, Mandler, and others [6, 16-29] (including our own [30-32]) have shown that, by coating electrodes with films that can amplify the electrochemical signal of a molecule of interest in the presence of other molecules with overlapping signals, such a semi-selective electrode can improve the selectivity of a single sensor in multicomponent mixtures. In one example from our previous work, we influenced the physicochemical properties of the redox reaction at the electrode by encapsulating carbon nanotubes (CNTs) in the pH-responsive bio-polymer chitosan, and showed that this modification decreased the standard redox potential of a molecule of interest due to the electrocatalytic nature of the CNTs [33]. However, despite these advances, the selectivity of such sensors is still far from being sufficient for discriminating between

individual molecules in multicomponent biological samples, because such samples often contain molecules with overlapping electrochemical signals, i.e., molecules whose electron-transfer rates during the redox reaction are too close to be differentiated by the modified electrode. Thus, to enable continuous monitoring of multiple diagnostic biological and chemical markers in biofluids, there is a critical need for novel approaches that can physically separate multiple redox-active molecules in a manner that will differentiate their electrochemical signals in the presence of other molecules with overlapping signals.

Biofabrication has been used to coat electrodes with films that can be further modified to functionalize the surface of the electrodes. The coating films usually consist of materials that are based on “stimuli-responsive polymers”, i.e., polymers that respond to various external stimuli such as pH, temperature, and more [13, 34-39]. These stimuli-responsive polymers facilitate a simple method for a high spatial resolution modification of microelectrodes and for their integration in miniaturized electrochemical sensors [40-43]. Specifically, the pH-responsive and functional bio-polymer chitosan has shown promising results for the thin film modification of microelectrodes [13, 14, 44-45]. Yet, the integration of chitosan as a functional biofabricated film for the modification of nanostructured electrodes has not been fully studied. To this end, the proposed study shows the modification of CNT arrayed electrodes with chitosan as a functional film for improved selectivity of electrochemical sensors.

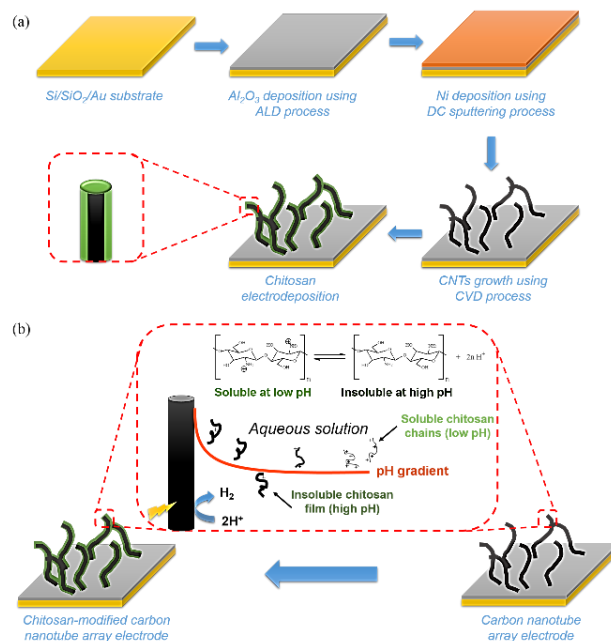
In this work, we biofabricated nanometers-scale thick chitosan films on top of CNT grown microfabricated electrodes. The CNTs were grown through a chemical vapor deposition (CVD) process while the chitosan was biofabricated using an electrodeposition process (Scheme 1a). The electrodeposition mechanisms is based on the increased pH that deprotonates the dissolved chitosan polymer, resulting in an electropolymerized chitosan film on an individual CNT (Scheme 1b). We characterized the morphology and the electrochemical activity of the CNT arrayed electrodes with and without the chitosan modification. We showed that the optimal growth of the CNT yielded effective surface area that was similar to a bare Au electrode. The modification with the chitosan enabled a functional surface, yet decreased the effective surface area by a factor of 5. Here, we demonstrate the feasibility to modify nanostructured electrodes with chitosan that can provide further modifications with functional molecules, such as enzyme or antibodies. That functionalization will enable the required selectivity for electrochemical sensing in multicomponent biofluids.

Experimental

Apparatus

Electrochemical studies were carried out using a 660D Potentiostat (CH Instruments, Inc. USA). A three-electrode system comprising of a microfabricated bare Au electrode modified with a CNT array and chitosan film as

a working electrode (methods for CNT growth and chitosan electrodeposition are described in the sub-section below). Ag/AgCl/3M KCl as a reference electrode and Pt wire as a counter electrode obtained from CH Instruments, Inc. (USA).



Scheme 1. Chitosan bio-modification of a carbon nanotube (CNT) arrayed electrode. (a) Fabrication steps of the chitosan-modified CNT arrayed electrode. (b) Chitosan electrodeposition mechanisms of an individual CNT.

Chemicals and reagents

All chemicals were purchased from Sigma-Aldrich and ultrapure water was used during all the electrochemical characterization process. A 1% chitosan solution was prepared from shrimp shells according to the previously described procedure in [31]. A 5 mM ferricyanide / 5 mM ferrocyanide mixture was prepared with a 10 mM phosphate buffer saline solution.

Microfabrication of the chitosan-modified carbon nanotube arrayed electrode

An array of CNTs was grown on a 0.5 cm² Au/Si/SiO₂ electrode that was microfabricated using a conventional photolithography process. First step for the growth of the CNT array on the Au electrode was the deposition of Al₂O₃ thin layer by thermal atomic layer deposition (ALD) process at 150°C, using TFS 500 reactor (BENEQ, Finland). This layer acts as a CVD catalyst diffusion barrier to prevent alloying with the Au during the pre-growth ripening process. After ALD, a Ni catalyst layer was deposited in an ATC 1800V sputtering system (AJA International Inc.). With the CVD catalyst layer in place, the samples were loaded into a low pressure chemical vapor deposition (LPCVD) system (Atomate Corp.) for the acetylene-based CNT growth process. Following the CNT array growth, a 0.5% chitosan solution was mixed with 2 wt % Pluronic F-127 (Sigma-Aldrich, USA) and

was ultrasonicated with the electrodes for 10 minutes following by an incubation period of 1 minute to improve the access of the CNT array to the chitosan. A current density of 6 A/m^2 was applied for 70 seconds to induce hydrolysis conditions. Finally, the chitosan-modified CNT arrayed electrode was incubated for 10 minutes in a 0.1 M phosphate buffer saline solution to remove excess of chitosan.

Electron microscopy characterization procedure

Electrode surface morphology studies were carried out using electron microscopy techniques. Scanning electron microscopy (SEM) characterization was done using SU-70 instrument (Hitachi, Germany). High resolution transmission electron microscopy (hr-TEM) characterization was conducted using JEM-2100 LaB6 instrument (JEOL, USA).

Electrochemical characterization procedure

The ferrocyanide/ferricyanide testing solution was incubated with the electrodes for 1 minute at open circuit potential conditions. Cyclic voltammograms were recorded between 0.46 V and -0.4 V vs Ag/AgCl for increasing scan rates of 0.025, 0.05, 0.08, and 0.1 V/s.

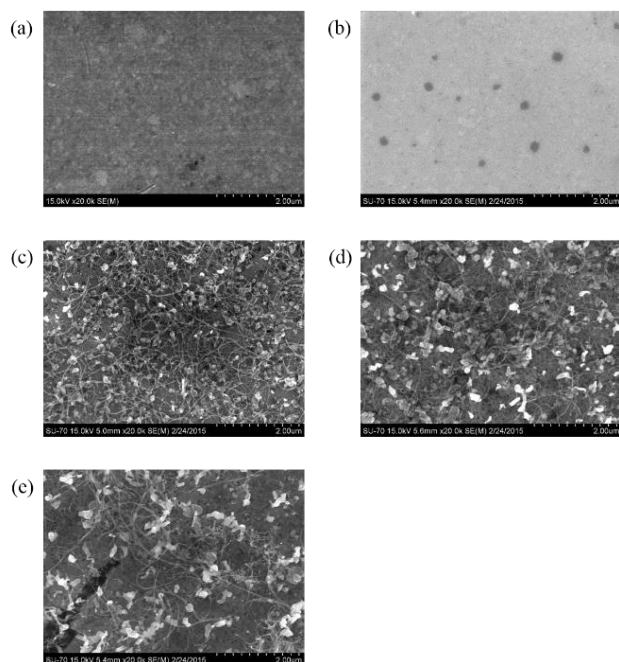


Fig. 1. Scanning electron micrographs of the different fabricated electrodes. a) Au, b) Au/Al₂O₃, c) Au/Al₂O₃/Ni(4nm)/CNTs, d) Au/Al₂O₃/Ni(7nm)/CNTs, and e) Au/Al₂O₃/Ni(10nm)/CNTs.

Results and discussion

Characterization of the carbon nanotubes growth

We optimized the thickness of the Ni catalyst film used for the CNT growth. We sputtered Ni films at thickness values of 4, 7, and 10 nm and characterized the resultant grown CNT array. **Fig. 1** shows scanning electron micrographs of the electrodes at the different microfabrication steps of the CNT growth. The obtained

micrographs demonstrated the presence of a CNT array without an apparent dependence on the thickness of the Ni layer. We deposited a film of Al₂O₃ between the Au and the Ni films to impede diffusion of Au atoms into the Ni [46-48], a process that may damage the purity of the film and its role as a catalyst for the CNT growth. Despite the increased resistivity of the Al₂O₃ diffusion barrier layer [49, 50] that decreased the intensity of the electrochemical currents, the conductivity of the CNT arrayed electrode was recovered (the electrochemical conductivity will be discussed in detail in the next sections).

Morphological study of the chitosan-modified carbon nanotube arrayed electrode

We characterized the structural morphology of the chitosan-modified CNT arrayed electrode using SEM and TEM. **Figs. 2(a, c) and 2(b, d)** show scanning electron micrographs of the CNT arrayed electrodes with and without the chitosan modification, respectively. While the CNT array alone was mostly adsorbed to the surface of the electrode, modification with chitosan maintained the three-dimensional structure of the array, which may be attributed to the chitosan film decreasing the adhesion forces between the Au electrode and the CNT. **Figs. 2e and 2f** show transmitting electron micrographs of the CNT arrayed electrodes with and without the chitosan modification, respectively. These micrographs revealed the diameter of the CNT (28.75 nm and 30.96 nm) that was bigger following the chitosan modification (56.80 nm).

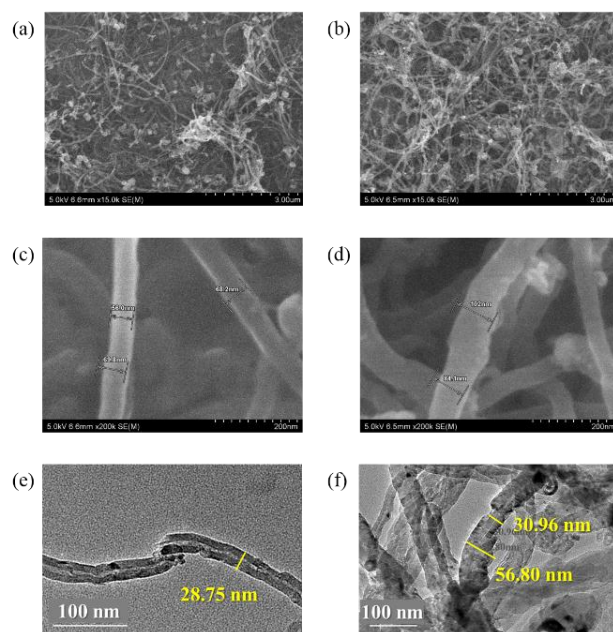


Fig. 2. Scanning and transmitting electron micrographs of either CNT alone (a, c, e) or CNT modified with chitosan (b, d, f).

Electrochemical characterization of the chitosan-modified carbon nanotube arrayed electrode

We characterized the electrochemical activity of the chitosan-modified CNT arrayed electrode by testing the

redox reaction of the conventional redox couple ferricyanide/ferrocyanide using the cyclic voltammetry electrochemical technique. All the electrodes showed reversible nernstian characteristics (Figs. 3a-e) and responded to faster scan rates by increasing electrochemical currents. The modified electrodes demonstrated lower currents than the unmodified Au electrode (Fig. 3f), which may be due to the increased charge transfer resistance donated by the Al_2O_3 diffusion barrier layer. Despite the decreased current characteristics of the modified electrodes, a 7 nm catalyst Ni layer resulted in currents that are close to the currents generated by the unmodified Au electrode, as opposed to the electrodes fabricated using 4 and 10 nm catalyst Ni layer (Fig. 3f).

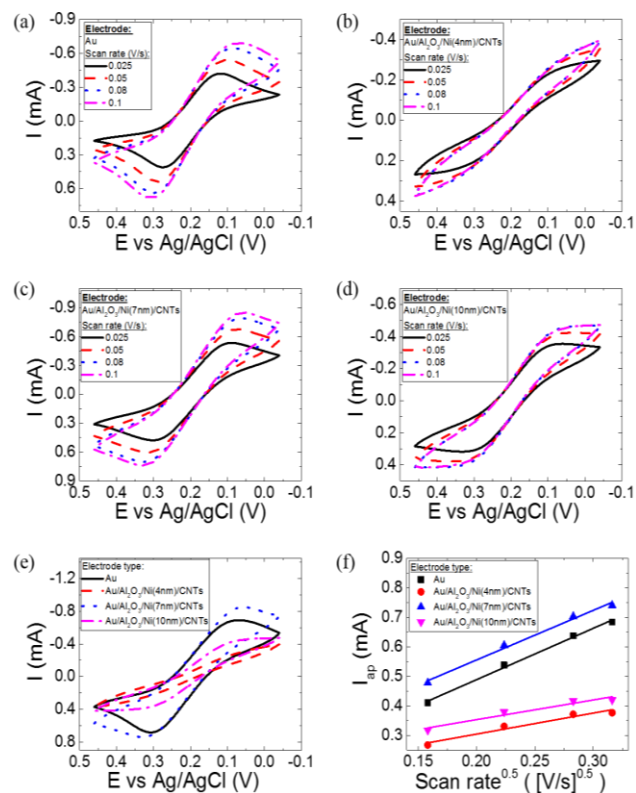


Fig. 3. Cyclic voltammograms at different scan rates of the different fabricated electrodes. a) Au, b) Au/ Al_2O_3 /Ni(4nm)/CNTs, c) Au/ Al_2O_3 /Ni(7nm)/CNTs, and d) Au/ Al_2O_3 /Ni(10nm)/CNTs. e) Comparison between the cyclic voltammograms recorded at 0.1 V/s scan rate with the different electrodes. f) Anodic current peak dependence on the scan rate of the cyclic voltammetry technique for the different electrodes.

The effective surface area (A_{eff}) can be calculated from the cyclic voltammograms using the Randles-Sevcik equation [51]:

$$i_p = 0.4463 \left(\frac{F^3}{RT} \right)^{1/2} n^{3/2} A_{eff} D^{1/2} C v^{1/2}$$

where, i_p is the peak current in Ampere, F is the Faraday's constant, R is the gas constant, T is the temperature in

Kelvin, n is the number of electrons transferred in the redox event (1 for ferricyanide/ferrocyanide redox reaction), A_{eff} is the electrode effective area in cm^2 , D is the diffusion coefficient in cm^2/s ($7.38 \cdot 10^{-6} \text{ cm}^2/\text{s}$ for ferricyanide [52]), and v is the scan rate in V/s . Table 1 shows the calculated A_{eff} for the different electrodes. Calculated A_{eff} values for electrodes fabricated using a 7 nm catalyst Ni layer resulted in bigger area ($0.46 \pm 0.03 \text{ cm}^2$) than using 4 nm ($0.19 \pm 0.03 \text{ cm}^2$) and 10 nm ($0.18 \pm 0.03 \text{ cm}^2$) catalyst Ni layers. Furthermore, A_{eff} of a 7 nm Ni layer was similar to those obtained with the unmodified Au electrode ($0.48 \pm 0.02 \text{ cm}^2$), demonstrating the recovery of the electrochemical activity of the modified electrode, which was aligned with our observation of the higher current characteristics (Fig. 3). Further modification with chitosan yielded a 5-times smaller A_{eff} than CNT array electrode without chitosan ($0.09 \pm 0.01 \text{ cm}^2$). The decreased A_{eff} may be due to the partially passivation of the electrode with the isolating chitosan while electrochemical activity is still present due to the porous structure of the chitosan [53].

Table 1. Comparison between the effective surface area (A_{eff}) calculated for different fabricated electrodes.

Electrode type	$A_{eff} (\text{cm}^2)$
Au	0.48 ± 0.02
Au/ Al_2O_3 /Ni(4nm)/CNTs	0.19 ± 0.03
Au/ Al_2O_3 /Ni(7nm)/CNTs	0.46 ± 0.03
Au/ Al_2O_3 /Ni(10nm)/CNTs	0.18 ± 0.03
Au/ Al_2O_3 /Ni/CNTs/Chitosan	0.09 ± 0.01

Conclusion

We presented a new method to functionalize nanostructured electrodes for the improved performance of electrochemical sensors. The approach is based on the electrodeposition of the functional bio-polymer chitosan to coat the CNT arrayed electrode. We demonstrated the targeted chitosan modification of individual CNTs in the array and the decreased electrochemical current due to the isolating chitosan.

The improved electrochemical activity of nanostructured microelectrodes is crucial for the reliable performance of miniaturized sensors due to their advantage of having a bigger surface area per volume properties. Further functionalization of the chitosan-modified nanostructures with specific receptors, such as enzymes and antibodies, will enable the required selectivity towards chemical and biological markers in multicomponent biofluids.

Acknowledgements

The authors would like to thank the Maryland NanoCenter and its FabLab.

Author's contributions

Conceived the plan: HB, MN; Performed the experiments: HB, MN, MS; Data analysis: HB; Wrote the paper: HB. Authors have no competing financial interests.

References

- Mishra, S.; Saadat, D.; Kwon, O.; Lee, Y.; Choi, W. S.; Kim, J. H.; Yeo, W. H.; *Biosens. Bioelectron.*, **2016**, *81*, 181-197.
DOI: [10.1016/j.bios.2016.02.040](https://doi.org/10.1016/j.bios.2016.02.040)
- Chen, Z.; Kim, J.; *BMC Urology*, **2016**, *16*(1), 11.
- Weltin, A.; Kieninger, J.; Urban, G. A.; *Anal. Bioanal. Chem.*, **2016**, *408*(17), 4503-4521.
DOI: [10.1007/s00216-016-9420-4](https://doi.org/10.1007/s00216-016-9420-4)
- Bandodkar, A. J.; Jia, W. Z.; Wang, J.; *Electroanalysis*, **2015**, *27*(3), 562-572.
DOI: [10.1002/elan.201400537](https://doi.org/10.1002/elan.201400537)
- Topkaya, S. N.; Azimzadeh, M.; Ozsoz, M.; *Electroanalysis*, **2016**, *28*(7), 1402-1419.
DOI: [10.1002/elan.201501174](https://doi.org/10.1002/elan.201501174)
- Sekretaryova, A. N.; Eriksson, M.; Turner, A. P. F.; *Biotechnol. Adv.*, **2016**, *34*(3), 177-197.
DOI: [10.1016/j.biotechadv.2015.12.005](https://doi.org/10.1016/j.biotechadv.2015.12.005)
- Katz, E.; *Electroanalysis*, **2016**, *28*(5), 904-919.
DOI: [10.1002/elan.201500635](https://doi.org/10.1002/elan.201500635)
- Bandodkar, A. J.; Wang, J.; *Trends Biotechnol.*, **2014**, *32*(7), 363-371.
DOI: [10.1016/j.tibtech.2014.04.005](https://doi.org/10.1016/j.tibtech.2014.04.005)
- Katz, E.; Fernandez, V. M.; Pita, M.; *Electroanalysis*, **2015**, *27*(9), 2063-2073.
DOI: [10.1002/elan.201500211](https://doi.org/10.1002/elan.201500211)
- Rochitta, G.; Spanu, A.; Babudieri, S.; Latte, G.; Madeddu, G.; Galleri, G.; Nuvoli, S.; Bagella, P.; Demartis, M. I.; Fiore, V.; Manetti, R.; Serra, P. A.; *Sensors (Basel)*, **2016**, *16*(6), 780.
DOI: [10.3390/s16060780](https://doi.org/10.3390/s16060780)
- Corrie, S. R.; Coffey, J. W.; Islam, J.; Markey, K. A.; Kendall, M. A.; *Analyst*, **2015**, *140*(13), 4350-4364.
DOI: [10.1039/c5an00464k](https://doi.org/10.1039/c5an00464k)
- Wang, J.; *Electroanalysis*, **2005**, *17*(1), 7-14.
DOI: [10.1002/elan.200403113](https://doi.org/10.1002/elan.200403113)
- Kim, E.; Xiong, Y.; Cheng, Y.; Wu, H. C.; Liu, Y.; Morrow, B. H.; Ben-Yoav, H.; Ghodssi, R.; Rubloff, G. W.; Shen, J. N.; Bentley, W. E.; Shi, X. W.; Payne, G. F.; *Polymers*, **2015**, *7*(1), 1-46.
DOI: [10.3390/polym7010001](https://doi.org/10.3390/polym7010001)
- Kim, E.; Liu, Y.; Ben-Yoav, H.; Winkler, T. E.; Yan, K.; Shi, X.; Shen, J.; Kelly, D. L.; Ghodssi, R.; Bentley, W. E.; *Adv. Healthc. Mater.*, **2016**, *5*(20), 2595-2616.
- Buffa, A.; Erel, Y.; Mandler, D.; *Anal. Chem.*, **2016**, *88*(22), 11007-11015.
DOI: [10.1021/acs.analchem.6b02827](https://doi.org/10.1021/acs.analchem.6b02827)
- Verma, A.; Fratto, B.; Privman, V.; Katz, E.; *Sensors*, **2016**, *16*(7), 1042. DOI: [10.3390/s16071042](https://doi.org/10.3390/s16071042)
- Guz, N.; Fedotova, T. A.; Fratto, B. E.; Schlesinger, O.; Alfonta, L.; Kolpashchikov, D. M.; Katz, E.; *ChemPhysChem*, **2016**, *17*(14), 2247-2255.
DOI: [10.1002/cphc.201600129](https://doi.org/10.1002/cphc.201600129)
- Katz, E.; Fratto, B. E.; Enzyme-Based Reversible Logic Gates Operated in Flow Cells, In *Advances in Unconventional Computing: Volume 2: Prototypes, Models and Algorithms*; Adamatzky, A. (Ed.); Springer International Publishing: Cham., **2017**, pp. 29-59.
DOI: [10.1007/978-3-319-33921-4_2](https://doi.org/10.1007/978-3-319-33921-4_2)
- Barsan, M. M.; Ghica, M. E.; Brett, C. M.; *Anal. Chim. Acta*, **2015**, *881*, 1-23.
DOI: [10.1016/j.aca.2015.02.059](https://doi.org/10.1016/j.aca.2015.02.059)
- Moreira, J. C.; Barek, J.; Wang, J.; *Sens. Electroanal.*, **2014**, *8*, 49-58.
- Walcarius, A.; Minteer, S. D.; Wang, J.; Lin, Y.; Merkoçi, A.; *J Mater. Chem. B*, **2013**, *1*(38), 4878-4908.
- Mishra, S.; Ashaduzzaman, M.; Mishra, P.; Swart, H. C.; Turner, A. P.; Tiwari, A.; *Biosens. Bioelectron.*, **2017**, *89*, 305-311.
- Parlak, O.; Turner, A. P.; *Biosens. Bioelectron.*, **2016**, *76*, 251-265.
- Parlak, O.; Beyazit, S.; Jafari, M. J.; Bui, B. T. S.; Haupt, K.; Tiwari, A.; Turner, A. P.; *Adv. Mater. Interf.*, **2016**, *3*(2), 1500353.
- Osikoya, A. O.; Parlak, O.; Murugan, N. A.; Dikio, E. D.; Moloto, H.; Uzun, L.; Turner, A. P. F.; Tiwari, A.; *Biosens. Bioelectron.*, **2017**, *89*, 496-504.
DOI: [10.1016/j.bios.2016.03.063](https://doi.org/10.1016/j.bios.2016.03.063)
- Parlak, O.; Incel, A.; Uzun, L.; Turner, A. P. F.; Tiwari, A.; *Bios. Bioelectron.*, **2017**, *89*, 545-550.
DOI: [10.1016/j.bios.2016.03.024](https://doi.org/10.1016/j.bios.2016.03.024)
- Turyan, I.; Khatwani, N.; Sosic, Z.; Jayawickreme, S.; Mandler, D.; *Anal. Biochem.*, **2016**, *494*, 108-113.
DOI: [10.1016/j.ab.2015.10.015](https://doi.org/10.1016/j.ab.2015.10.015)
- Hitrik, M.; Pisman, Y.; Wittstock, G.; Mandler, D.; *Nanoscale*, **2016**, *8*(29), 13934-13943.
- Ratner, N.; Mandler, D.; *Anal. Chem.*, **2015**, *87*(10), 5148-5155.
DOI: [10.1021/ac504584f](https://doi.org/10.1021/ac504584f)
- Ben-Yoav, H.; Chocron, S. E.; Winkler, T. E.; Kim, E.; Kelly, D. L.; Payne, G. F.; Ghodssi, R.; *Electrochim. Acta*, **2015**, *163*, 260-270.
- Ben-Yoav, H.; Winkler, T. E.; Kim, E.; Chocron, S. E.; Kelly, D. L.; Payne, G. F.; Ghodssi, R.; *Electrochim. Acta*, **2014**, *130*, 497-503.
- Kim, E.; Chocron, S. E.; Ben-Yoav, H.; Winkler, T. E.; Liu, Y.; Glassman, M.; Wolfram, C.; Kelly, D. L.; Ghodssi, R.; Payne, G. F.; *Adv. Funct. Mater.*, **2015**, *25*(14), 2156-2165.
DOI: [10.1002/adfm.201403783](https://doi.org/10.1002/adfm.201403783)
- Shukla, S. K.; Lavon, A.; Shmulevich, O.; Ben-Yoav, H., *Carbon Nanotubes Biopolymer Based Biosensor for the Electrochemical Detection of Neurotransmitters, in Israel Vacuum Society 34th Annual Conference, 2016*: Beer Sheva, Israel.
- Zhou, J.; Sheiko, S. S.; *J Polym. Sci. Part B Polym. Phys.*, **2016**, *54*(14), 1365-1380.
DOI: [10.1002/polb.24014](https://doi.org/10.1002/polb.24014)
- Zhang, K. Y.; Liu, S. J.; Zhao, Q.; Huang, W.; *Coord. Chem. Rev.*, **2016**, *319*, 180-195.
DOI: [10.1016/j.ccr.2016.03.016](https://doi.org/10.1016/j.ccr.2016.03.016)
- Xu, Q. H.; He, C. L.; Xiao, C. S.; Chen, X. S.; *Macromol. Biosc.*, **2016**, *16*(5), 635-646.
DOI: [10.1002/mabi.201500440](https://doi.org/10.1002/mabi.201500440)
- Wang, Y.; Feng, A. C.; Yuan, J. Y.; *Prog. Chem.*, **2016**, *28*(7), 1054-1061.
DOI: [10.7536/pc160217](https://doi.org/10.7536/pc160217)
- Ferreira, A.; Novoa, P. R. O.; Marques, A. T.; *Compos. Struct.*, **2016**, *151*, 3-35.
DOI: [10.1016/j.compstruct.2016.01.028](https://doi.org/10.1016/j.compstruct.2016.01.028)
- Liu, L.; Mandler, D. (Eds.); *The Sol-Gel Handbook: Synthesis, Characterization and Applications, 3-Volume Set*; **2015**.
- Florea, L.; Dunne, A.; Francis, W.; Bruen, D.; Tudor, A.; Diamond, D.; *Stimuli-responsive Materials for Self-reporting Micro-fluidic Devices, in IC-ANMBES, 2016*: Brasov, Romania.
- Manrique-Juárez, M. D.; Rat, S.; Salmon, L.; Molnár, G.; Quintero, C. M.; Nicu, L.; Shepherd, H. J.; Bousseksou, A.; *Coord. Chem. Rev.*, **2016**, *308*, 395-408.
- Gamella, M.; Zakharchenko, A.; Guz, N.; Masi, M.; Minko, S.; Kolpashchikov, D. M.; Iken, H.; Poghosian, A.; Schöning, M. J.; Katz, E.; *Electroanalysis*, **2016**, *28*, 1-12.
DOI: [10.1002/elan.201600389](https://doi.org/10.1002/elan.201600389)
- Parlak, O.; Beyazit, S.; Tse-Sum-Bui, B.; Haupt, K.; Turner, A. P. F.; Tiwari, A.; *Nanoscale*, **2016**, *8*(19), 9976-9981.
DOI: [10.1039/c6nr02355j](https://doi.org/10.1039/c6nr02355j)
- Yi, H.; Wu, L.-Q.; Bentley, W. E.; Ghodssi, R.; Rubloff, G. W.; Culver, J. N.; Payne, G. F.; *Biomacromolecules*, **2005**, *6*(6), 2881-2894.
- Koef, S.; Dykstra, P.; Luo, X.; Rubloff, G.; Bentley, W.; Payne, G.; Ghodssi, R.; *Lab Chip*, **2010**, *10*(22), 3026-3042.
- Pinnel, M. R.; Bennett, J. E.; *Metall. Trans. A*, **1976**, *7*(5), 629-635.
DOI: [10.1007/bf03186793](https://doi.org/10.1007/bf03186793)
- Rairden, J. R.; Neugebauer, C. A.; Sigsbee, R. A.; *Metall. Trans.*, **1971**, *2*(3), 719-722.
DOI: [10.1007/bf02662726](https://doi.org/10.1007/bf02662726)
- Ziegler, J.; Baglin, J.; Gangulee, A.; *Appl. Phys. Lett.*, **1974**, *24*, 36.
- Hoex, B.; Schmidt, J.; Pohl, P.; Van de Sanden, M.; Kessels, W.; *J Appl. Phys.*, **2008**, *104*(4), 044903.
- Huang, M.; Chang, Y.; Chang, C.; Lee, Y.; Chang, P.; Kwo, J.; Wu, T.; Hong, M.; *Appl. Phys. Lett.*, **2005**, *87*(25), 252104.
- Bard, A. J.; Faulkner, L. R., *Electrochemical Methods: Fundamentals and Applications, 2nd Edition* ed. **2001**: Wiley, 864.
- Konopka, S. J.; McDuffie, B.; *Anal. Chem.*, **1970**, *42*(14), 1741-1746.
DOI: [10.1021/ac50160a042](https://doi.org/10.1021/ac50160a042)
- Bellich, B.; D'Agostino, I.; Semeraro, S.; Gamini, A.; Cesaro, A.; *Mar Drugs*, **2016**, *14*(5), 99.
DOI: [10.3390/md14050099](https://doi.org/10.3390/md14050099)